THE ASTROPHYSICAL JOURNAL, 412:213–221, 1993 July 20

QUARK NEUTRON LAYER STARS

PHILIP A. CARINHAS
Department of Physics, University of Wisconsin, Milwaukee, Wisconsin 53201
Received 1992 November 16; accepted 1993 February 1

ABSTRACT

Typical nuclear equations of state and a quark bag model, surprisingly, allow compact stars with alternate layers of neutrons and quarks. One can determine on the basis of the Gibbs free energy which phase, nuclear or quark, is energetically favorable. Using the nuclear equation of state of Wiringa, and a quark equation of state given by Freedman and McLerran, the allowed quark parameter space for such layer stars is searched. This paper differs from past work in that configurations are found in which quark matter is located exterior and interior to shells of nuclear matter, i.e., dependent on quark parameters, a star may contain separate layers of quark and nuclear matter. Given the uncertainty in the quark parameter space, one can estimate the probability for finding pure neutron stars, pure quark stars (strange stars), stars with a quark core and a nucleon exerior, or layer stars. Several layer models are presented. The physical characteristics, stability, and results of a thorough search of the quark parameter space are presented.

Subject headings: elementary particles — equation of state

1. INTRODUCTION

Although compact stars are thought to be composed of neutrons, there is still no compelling evidence for the microscopic description of matter in them, partly because of the difficulty in experimentation at extreme densities.

Recently, there has been a great interest in QCD phase transitions and the composition of compact stars, including quark stars, strange stars, neutron stars with pion condensate, gluon condensate, and quarks (Benvenuto, Horvath, & Vucetich 1991; Campbell, Ellis, & Olive, 1990; Ellis, Kapusta, & Olive 1991; Grassi 1989; Haensel, Zdunik, & Schaeffer 1986).

This paper investigates the possibility that dense stars with more than one layer of neutron matter and quark matter exist. If the Witten hypothesis is correct, the ground state of matter may be strange, hence, dense stars with these structures could occur in nature (Witten 1984).

The Wiringa (Wiringa et al. 1988) equation of state and a quark equation of state given by Freedman and McLerran are used (Freedman and McLerran 1978). Given this and the possible quark parameter range, stars which have separate layers of neutron and quark matter are constructed. For a maximum and a minimum pressure, the quark parameter space is classified according to the most complex structure that can be constructed from these parameters. The fractional volumes of the quark parameter space for each stellar type are calculated. Given the uncertainty in the quark parameters, there is a finite area in the quark parameter space for which layer stars can exist.

This work assumes two phases of matter that are each electrically neutral. This leads to a discontinuous quark-neutron phase transition, with discontinuities in the energy and mass densities. Glendenning (1992) has recently argued that if one requires only overall neutrality, allowing two intermixed phases to each have a net charge, the phase transition from nucleon matter to quark matter can occur gradually over a finite range of pressure. The energy density and chemical potentials would be continuous through the transition region. Although Glendenning has neglected surface effects of the two embedded phases, the general features of the mixed phase described there should not change. Note that some of the phase transitions which occur in the current work (that are close in pressure) would likely be part of a single mixed phase region under Glendenning's assumptions.

2. QUARK PARAMETERS AND THE BAG MODEL

In this section, a version of the bag model due to Freedman and McLerran 1978) is introduced, and the relevant bounds on the quark parameter space are discussed. Strange matter is modeled as a degenerate Fermi gas of u, d, and s quarks and electrons (positrons). Chemical equilibrium between the three flavors is maintained by the reactions:

$$\begin{aligned} d &\rightarrow u + e + \bar{\nu}_e \,, \\ u + e &\rightarrow d + \nu_e \,, \\ s &\rightarrow u + e + \bar{\nu}_e \,, \\ s + u &\leftrightarrow d + u \,. \end{aligned} \tag{1}$$

The chemical potentials of the lost neutrinos are set to zero since they interact very weakly. It is assumed that the strange quark has a mass $m_s = m$, and no gluon exchange is considered. The above reactions imply that

$$\mu_d = \mu_s \equiv \mu \,, \quad \mu_u + \mu_e = \mu \,. \tag{2}$$

Overall charge neutrality for bulk matter implies

$$2n_u - n_d - n_s - 3n_e = 0 \,, \tag{3}$$

where the number densities are given in terms of the thermodynamic potentials Ω_a ($a = u, d, s, e$) given in the Appendix,

$$n_a = -\frac{\partial \Omega_a}{\partial \mu_a} \,. \tag{4}$$

A consequence of equations (1) and (3) is that only one chemical potential is left independent. The energy density of the fermions is $\Sigma_a(\Omega_a + n_a \mu_a)$. The vacuum associated with bulk

quark matter is also assumed to contain a positive energy per volume, called the bag energy, denoted by B. The total energy density is therefore

$$\epsilon = \sum_a (\Omega_a + n_a \mu_a) + B \, . \tag{5}$$

The quark parameters are then given by α_c (the strong coupling constant of QCD), m_s, and the bag constant B. There is also another parameter, the renormalization point ρ_r which is given the constant value of $\rho_r = 313$ MeV. See Alcock et al. (1986) for a discussion of this value. There are effectively three parameters to consider. The baryon number density is given by $n_A = \frac{1}{3}(n_u + n_d + n_s)$. Chemical equilibrium between the Fermi pressure and vacuum pressure is achieved via

$$\frac{\partial}{\partial \mu} (\epsilon / n_A) = 0 \, . \tag{6}$$

Equivalently,

$$\sum_a \Omega_a = -B \, . \tag{7}$$

For known values of B and m, one can solve for μ in equation (6), yielding equilibrium number densities and energy densities and the energy per baryon. Curves of constant E/A are calculated (numerically) and determine the value of $B^{1/4}$ for which nonstrange quark matter has an energy per baryon of $930 + \Delta$ MeV. To the left of this line, nuclei with high atomic numbers are unstable against decay into nonstrange quark matter. The quantity Δ, determined in Farhi and Jaffe (1984), is due to shell effects in nuclei, and the value 930 is the energy per baryon for the most stable nuclei, viz., iron. The allowed values of $B^{1/4}$ narrow as m_s increases, as can be seen in Figure 1. This places lower limits on B as a function of α_c. There is no similar argument for an upper limit on B, or the other quark parameters.

Since we are using a perturbative expansion in powers of α_c, one must be skeptical of the quark equation of state in a regime where $\alpha_c \geqslant 1$. For $\alpha_c > 1.0$, second-order contributions in α_c^2 are greater than the zero-order result, and the energy density is unbounded from below as $T \to \infty$ (Chin 1978). The typical energy scale of neutrons stars is also well below that of deconfinement when the bag model is appropriate. Despite these considerations, results up to $\alpha_c = 1.5$ (where the equation of state becomes unstable) are included. Some limits on values for the quark parameters are given by several authors in Table 1. The first four references come from fits to heavy ion experiments. The last values are those used by the author.

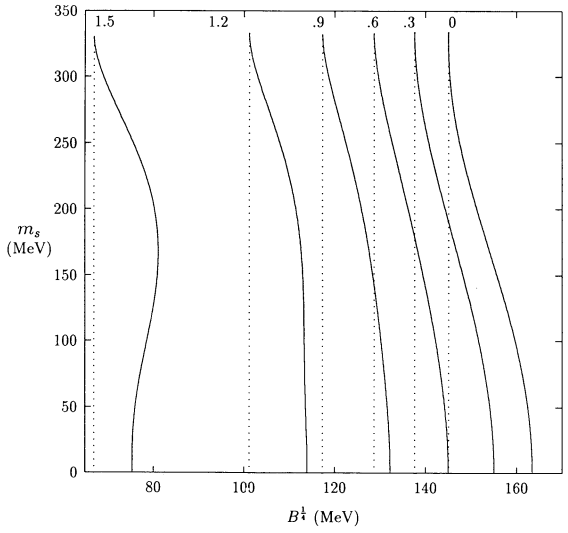

FIG. 1.—Curves of constant $E/A = 934$ MeV. The value of α_c is given by the label at the top of each curve. The dotted lines indicate the minimum value, $B_{\min}$, allowed.

TABLE 1

RANGE OF QUARK PARAMETERS

Reference	α_c	m_s (MeV)	$B^{1/4}$(MeV)
Benvenuto et al. 1991	0.5–0.6	150–200	145
DeGrand et al. 1975	2.2	280	145
Bartelski et al. 1984	2.0	283	149
Chanowitz et al. 1983	2.8	340	120
Carlson et al. 1983	≤ 1.0	288	$\sim$200–220
This paper	0–1.5	0–330	$B_{\min}$–240

3. PHASE TRANSITIONS AND LAYER STARS

This section discusses the construction and physical characteristics of layer stars. The matter type is determined by the Gibbs free energy criterion for two competing types of matter. The structure of layer stars is examined and is compared to known stellar models.

Consider the Wiringa equation of state and the quark bag equation of state, assuming for the moment that quark matter is stable at the core. The Oppenheimer-Volkoff (OV) equations governing hydrodynamic equilibrium are

$$\frac{dm}{dr} = 4\pi r^2 \epsilon \, ,$$

$$\frac{dP}{dr} = -\frac{1}{r} \frac{(P + \epsilon)(m + 4\pi P r^3)}{(r - 2m)} \, , \tag{8}$$

where m is the mass interior to radius r, P is pressure, and r is the radial coordinate. Numerical integration of these equations for spherical stars is outlined in Shapiro and Teukolsky (1983, p. 23).

At each step of integration, calculate the Gibbs free energy per baryon,

$$g = \frac{\epsilon + P}{n} \, . \tag{9}$$

(It is assumed that T is small compared to the Fermi energy of the matter, and so T and s can be neglected.) Label quark matter as "Q" and nuclear matter as "N". When the Gibbs free energy of quark matter surpasses (for the same pressure) the Gibbs free energy of nuclear matter, the equation of state (or table) is changed to that of nuclear matter. This point represents the phase transition between the two materials. The OV equations are then integrated with the new equation of state until the pressure drops to zero and the program terminates. The number and hence the energy density are not continuous at the phase transition; however, g and P are continuous everywhere. The hybrid case has been studied for first- and second-order phase transitions using a mean field equation of state (Ellis et al. 1991).

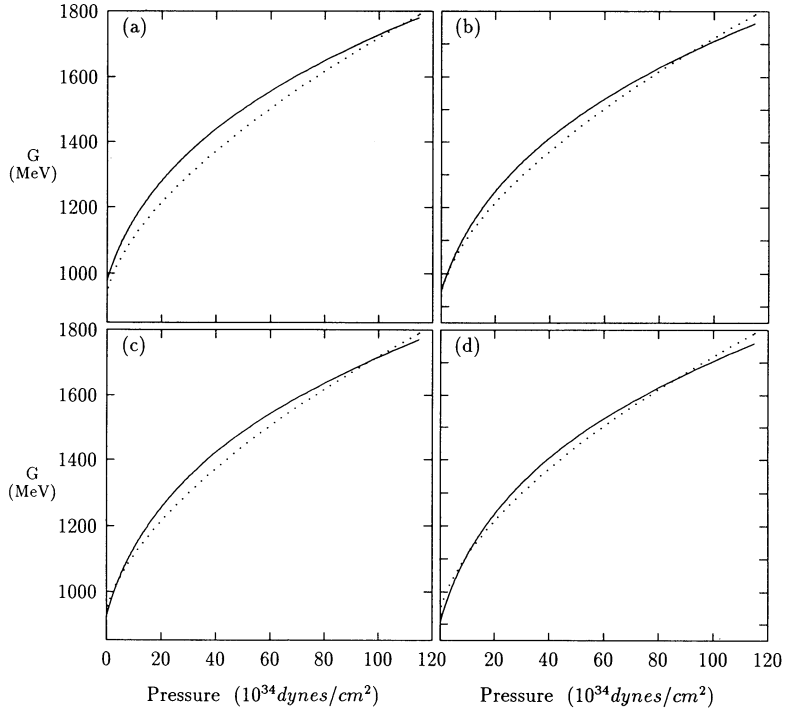

FIG. 2.—Gibs free energy vs. pressure for layer stars. (*a*) $\alpha_c = 0.5$, $m_s = 300$ MeV, $B^{1/4} = 140$ MeV; (*b*) $\alpha_c = 0.5$, $m_s = 220$ MeV, $B^{1/4} = 140$ MeV; (*c*) $\alpha_c = 0.5$, $m_s = 280$ MeV, $B^{1/4} = 132$ MeV; (*d*) $\alpha_c = 0.5$, $m_s = 230$ MeV, $B^{1/4} = 132$ MeV. Dotted lines correspond to the Wiringa equation of state.

If the quark parameters are such that the quark equation of state crosses the neutron equation with the neutron equation of state having lower Gibbs free energy at low pressure, nucleons will be the stablest at low energy (at the surface of the star). If the Gibbs free energy of the quark matter is lower at low pressure, one will have quark matter at the surface.

This paper considers stars which have any type of matter at the core or surface, and have a number of layers of matter which alternate between quark and neutron. The Gibbs free energy as a function of pressure is presented below for four choices of quark parameters B, m_s, and α_c in Figure 2.

For the choice of parameters, Figure 2*a* yields a star which has one phase transition at pressure $P = 108.7 \times 10^{34}$ dynes/cm^{-2}; Figure 2*b* has three crossings at $P = 0.556$, 2.81, and 89.46×10^{34} dynes/cm^{-2}; Figures 2*c* and 2*d* both have two crossings at 4.91, 97.26, and 10.43, 86.99×10^{34} dynes/cm^{-2}, respectively. The central pressure is that for the maximum mass Wiringa model.

3.1. *Quark Neutron Layer Stars*

Consider sequences based on the parameters in the previous section. The following mass-radius and moment of inertia-radius diagrams (Fig. 3) contain all the essential features of layer stars for both models with quark exteriors and neutron exteriors. Note the similarity between a pure neutron sequence and the cases given in Figures 3*a* and 3*b*, and that between pure quark sequences and the cases given in Figure 3*c* and 3*d*.

The sequence given in Figure 3*a* has the appearance of a pure neutron mass-radius diagram, except for the peak at the onset of the QN phase. Also, in Figure 3*b* the QN region is drawn into a smaller radius as compared to the pure neutron part of sequence in Figure 3*a*. This is due to the presence of a quark core in the QN models. For phase transition which occur at lower pressures, this feature is enhanced to the point of meeting the pure quark sequences at low mass. The onset of instability often coincides with a phase transition from neutron to quark matter. This is due to the quark equation of state being softer than the neutron equation of state at these pressures. Figure 4*a* most closely resembles a pure neutron sequence. Figure 4*b* has a much smaller radius at low moment of inertia, resembling Figures 4*c* and 4*d*, as in pure quark sequences. This is similar to the mass-radius diagrams in Figure 3.

Accuracy for the stellar calculations were checked against constant density star models (which are exactly solvable) to better than 3.0×10^{-6}% for the radius and 1.5×10^{-3}% for the mass.

3.2. *Layer Star Profiles*

Figures 5–7 show the physical parameters for four layer stars as a function of radius of the star. In all cases, the central pressure is chosen to be that for the maximum mass Wiringa model, $P_c = P_{max} = 1.15 \times 10^{34}$ dynes cm^{-2}. The energy density is discontinuous at phase transitions; however, the pressure and mass remain continuous throughout the star. In Figures 5*a* and 5*b* the matter is originally in the neutron phase and then is in the Q-phase after the first discontinuity. There are no other transitions in Figure 5*a*; however, Figure 5*b* undergoes two more transitions to N and Q, respectively. The models given in Figures 5*c* and 5*d* both go through a Q, N, and Q phase.

The pressure-radius diagrams are continuous with a flattening in Figures 6*a* and 6*b* at low pressure due to the stiff nuclear equation of state at low pressure. The mass-radius profiles are more interesting. Figures 7*a* and 7*b* are flat near the surface, again due to the stiff nuclear equation of state at low

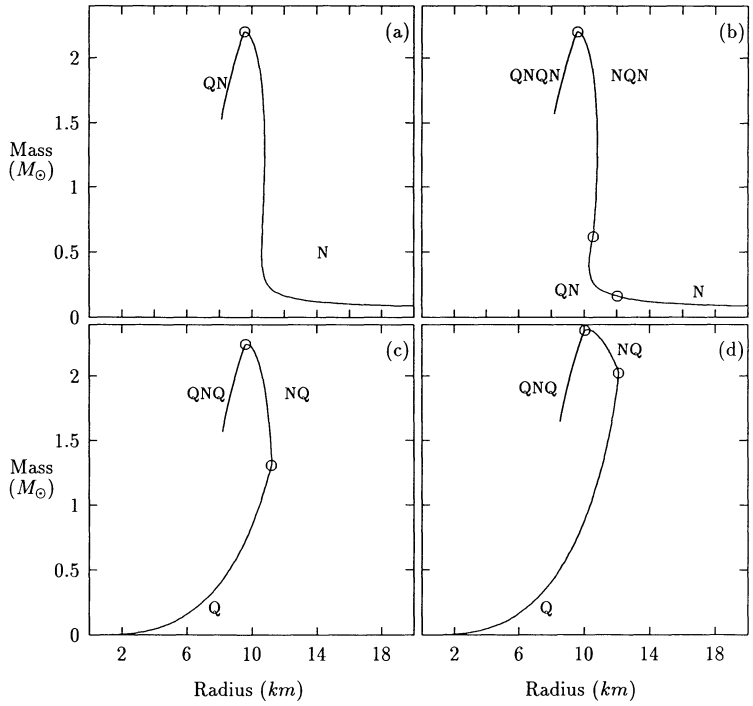

FIG. 3.—Mass vs. radius and moment of inertia vs. radius for layer stars. Circles in the sequences correspond to phase transition from one stellar type to the next. Quark parameters are given in Fig. 2 (legend).

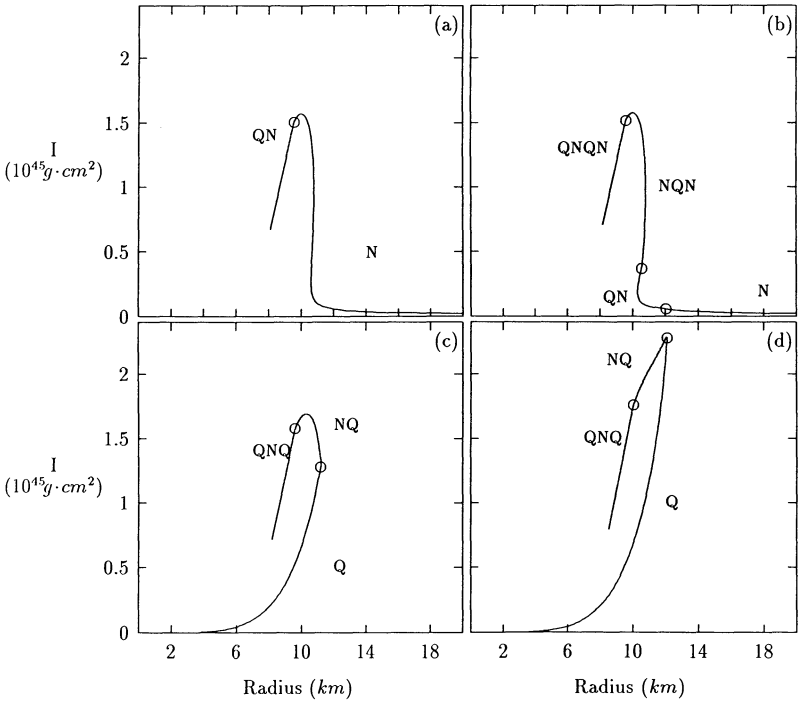

FIG. 4.—Moment of inertia vs. radius and moment of inertia vs. radius for layer stars. Circles correspond to phase transition as in Fig. 3. Quark parameters are as in Fig. 2.

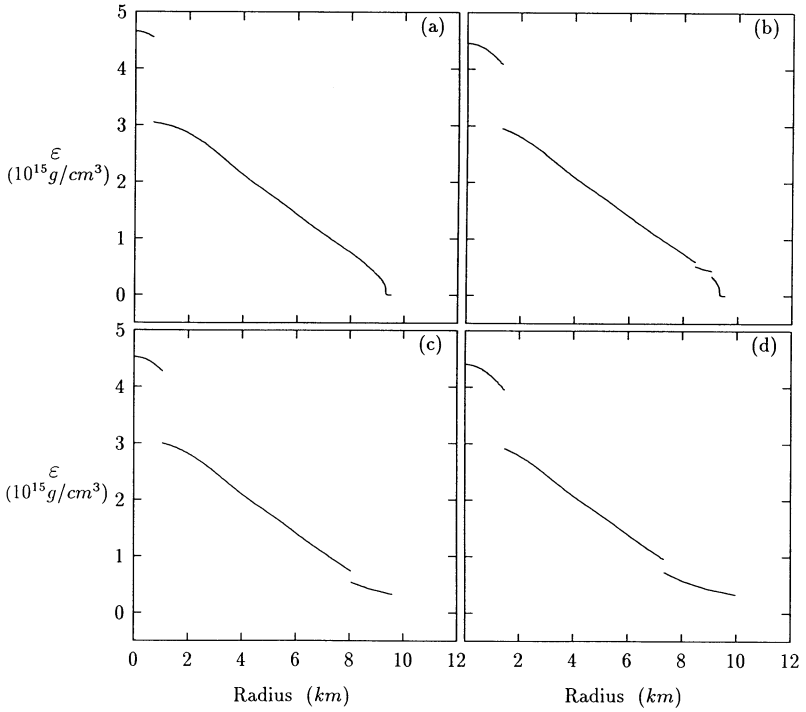

FIG. 5.—Energy density–radius profile for layer stars. Discontinuities in the plots correspond to the phase transition from one type of matter to the next. Quark parameters are as in Fig. 2.

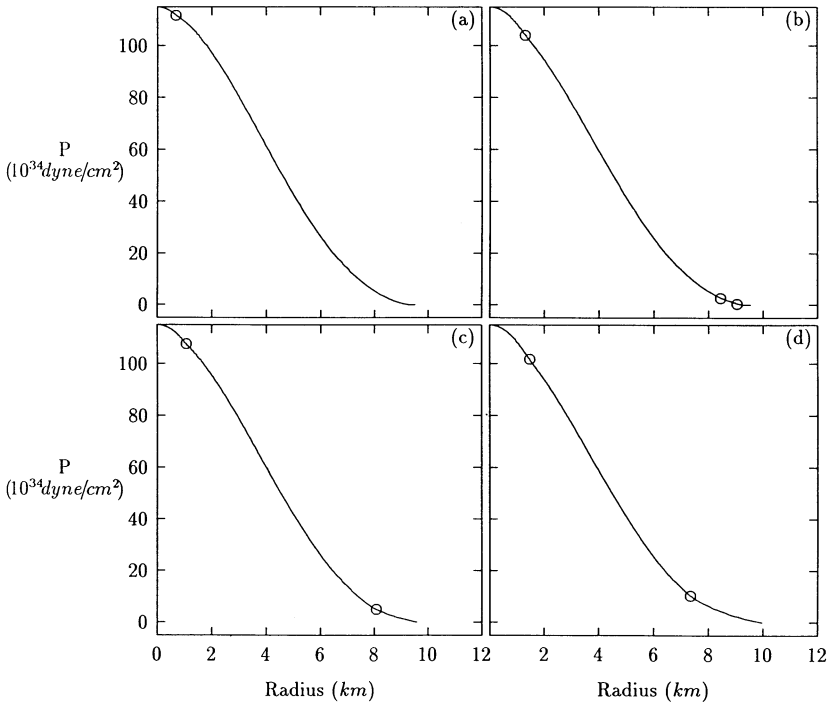

FIG. 6.—Pressure-radius profile for layer stars. Circles in the sequences mark phase transitions from one stellar type to the next. Quark parameters are as in Fig. 2.

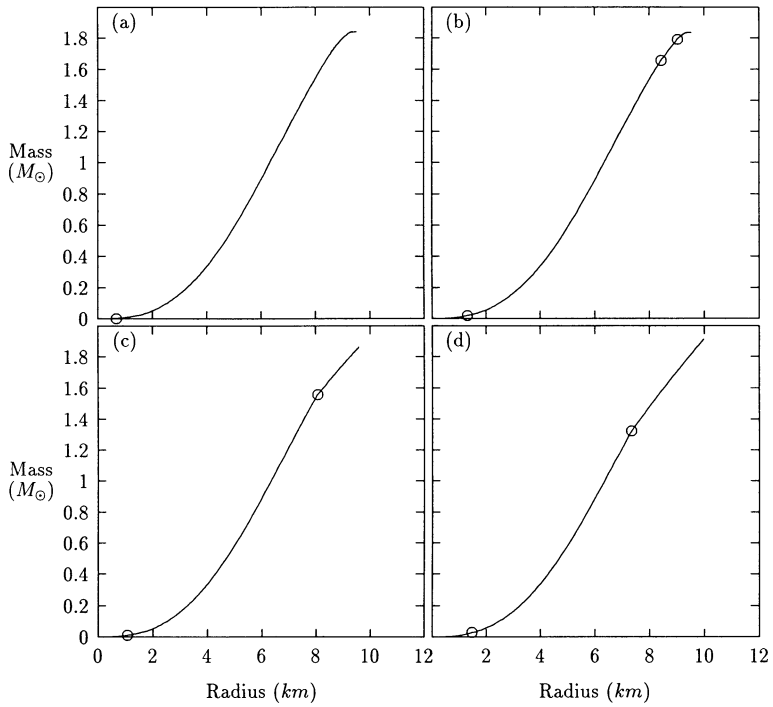

FIG. 7.—Mass-radius profiles for layer stars. Circles in the sequences mark phase transitions from one stellar type to the next. Quark parameters are as in Fig. 2.

pressure. Figures 7*c* and 7*d* are almost linear in the quark phase in the exterior region.

4. QUARK PARAMETER SPACE FOR Q–N LAYER STARS

This section discusses the classification of that part of the quark parameter space that is consistent with current knowledge of the quark parameters. The quark parameter space is classified according to the number of phase changes that occur between $P_{\min}$ to $P_{\max}$, with special regard for the order in which the phase of matter, neutron or quark, appears. $P_{\min}$ is chosen at the pressure corresponding to the energy density where neutron drip occurs, $\rho_{\rm ND} \sim 4.54 \times 10^{12}$ g cm^{-3} which corresponds to $P_{\min} \sim 7.0 \times 10^{29}$ dyne cm^{-3} for the Wiringa equation of state. $P_{\min} = 1.0 \times 10^{30}$ dyne cm^{-3} is taken as the more conservative value. $P_{\max}$ is taken as the pressure corresponding to the onset of instability for the neutron regime of the Wiringa equation of state. Associate to that point in the quark parameter space a sequence of Q's and N's, corresponding to the matter phase of the layers emanating from the core of the star to the exterior. A neutron core and a quark exterior would be labeled as a "NQ" for example.

4.1. *Calculation of the Parameter Space*

For each point in the (α_c, m_s) plane of dimensions $\delta\alpha_c \times \delta m_s = 0.01 \times 3.0$ MeV, the minimum and maximum value of $B^{1/4}$ for each stellar type is calculated to an accuracy of $\Delta B = 0.03$ MeV.

The volume of stellar type A in the quark parameter space, V_A, is calculated as

$$V_A \sim \sum_i \Delta\alpha_{c_i} \Delta m_{s_i} (B_{A+} - B_{A-})_i = \Delta\alpha_c \, \Delta m_s \sum_i hB_{Ai} , \quad (10)$$

where $hB_{Ai} = (B_{A+} - B_{A-})_i$ is the height of the ith space that corresponds to that point in the quark parameter space, and $\Delta\alpha_c$, Δm_s are constants. The uncertainty in B is taken as half of the accuracy in B, $\delta B_A = \frac{1}{2}\Delta B$. Given that $\delta(B_{A+} - B_{A-})_i = 2\delta B_{Ai} = \Delta B$, the uncertainty δV_A is similarly calculated as

$$\delta V_A \sim \Delta\alpha_c \, \Delta m_s \sum_i \delta hB_{Ai} = \Delta\alpha_c \, \Delta m_s \sum_i \delta(B_{A+} - B_{A-})_i$$
$$= \Delta\alpha_c \, \Delta m_s \sum_i \Delta B_{Ai} . \quad (11)$$

From the results of this calculation one can determine the relative volumes of parameter space of each stellar class. The results are summarized in Table 2. N and QN occupy the majority of the entire space (see Fig. 8). This is due in part to the monotonicity of the equations of state and to the fact that the nuclear equation of state usually dominates at low pressures.

The other components of the quark parameter space are much smaller and are illustrated in Figures 9–11. Figure 9 shows the next two largest spaces, NQN and NQ, which together occupy about 4.4% of the quark parameter space. The NQN space occurs precisely above (in the $B^{1/4}$ axis), the NQ space as a result of phase transitions at low pressure (density). NQN is very thin in $B^{1/4}$, as can be seen in Figure 9*a*. This is due to two phase transitions which occur at low pressure. Figure 10*a* and 10*b* show the next two largest spaces, QNQ and QNQN, which occupy about 1.3% of the quark parameter

TABLE 2

SUMMARY OF PARAMETER SPACE CLASSIFICATION

Class	V_i/V	$\Delta V_i/V$
N	0.735	0.008
QN	0.176	0.004
Q	0.021	0.002
NQ	0.045	0.005
QNQ	0.009	0.001
NQN	0.006	0.005
QNQN	0.006	0.002

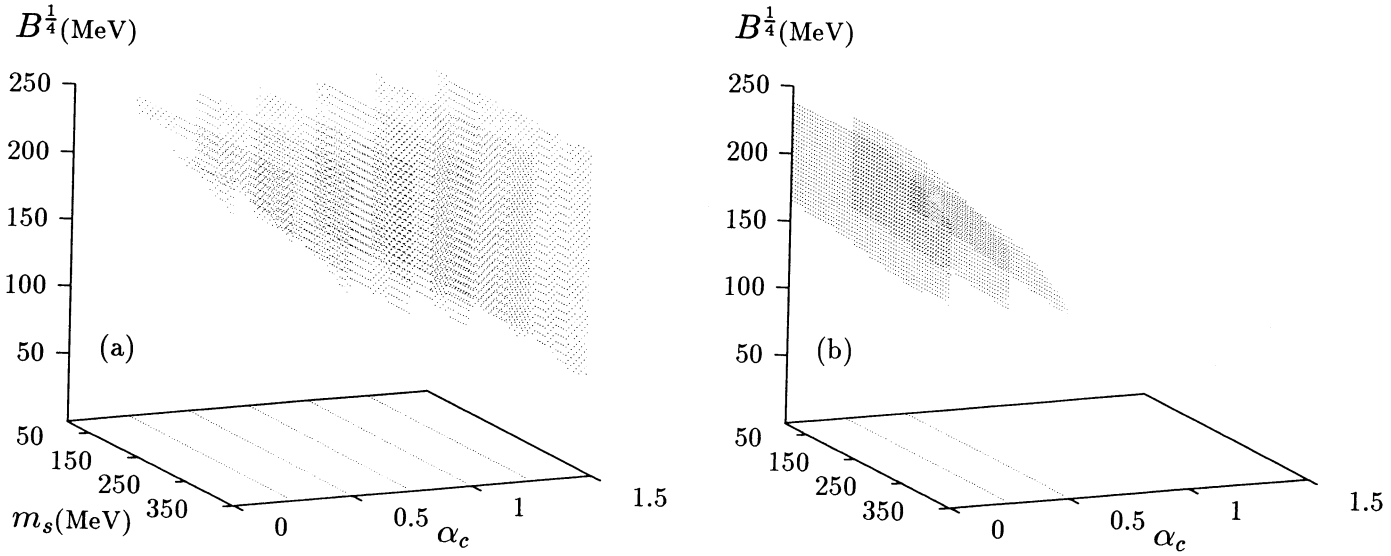

FIG. 8.—(*a*) Parameter space for neutron (N) stars. (*b*) Parameter space for QN stars. Slices are plotted at increments of $\alpha_c = 0.25$. These two spaces comprise over 90% of the total quark parameter space.

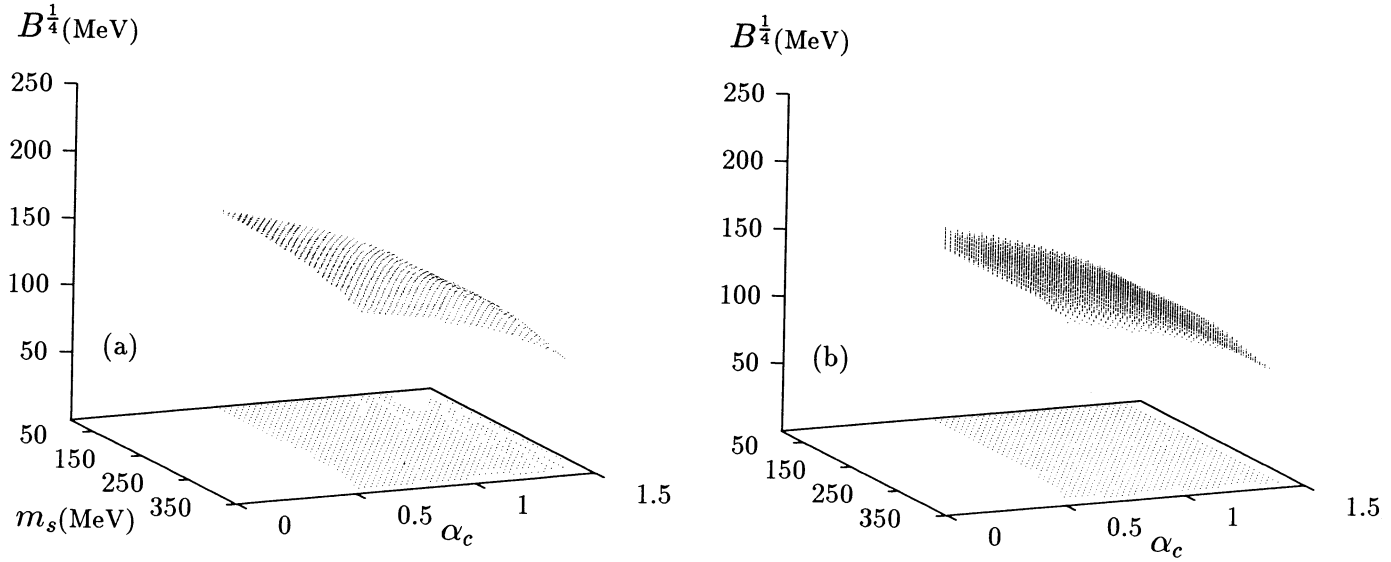

FIG. 9.—(*a*) Parameter space for NQN stars and (*b*) for NQ stars

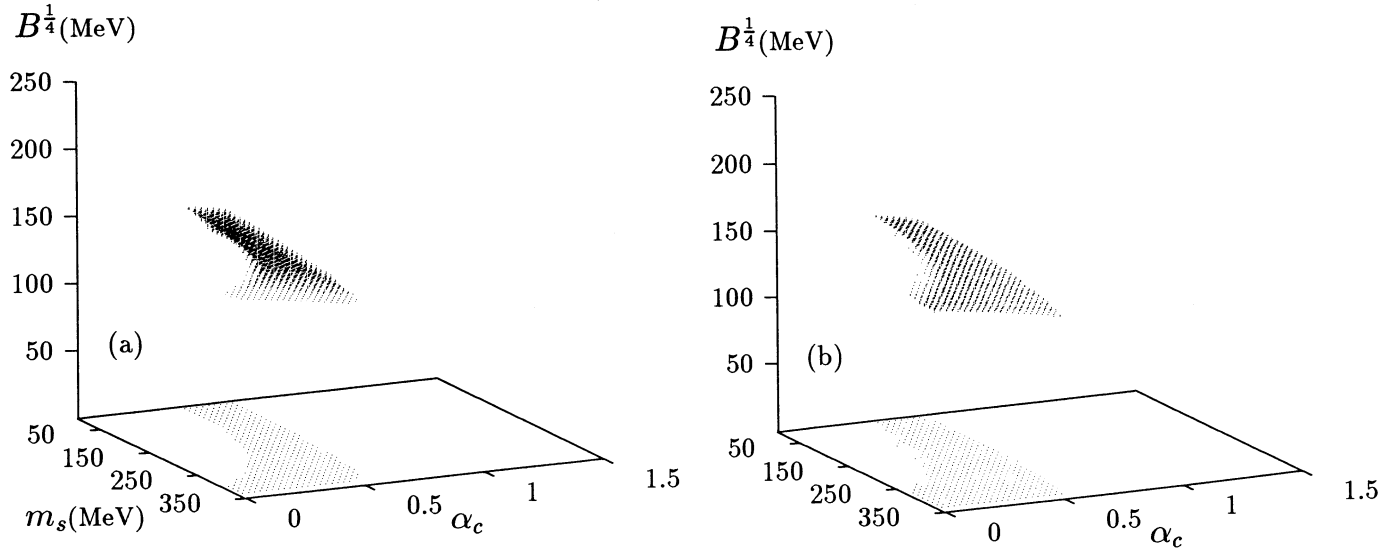

FIG. 10.—(*a*) Parameter space for QNQ stars and (*b*) for QNQN stars

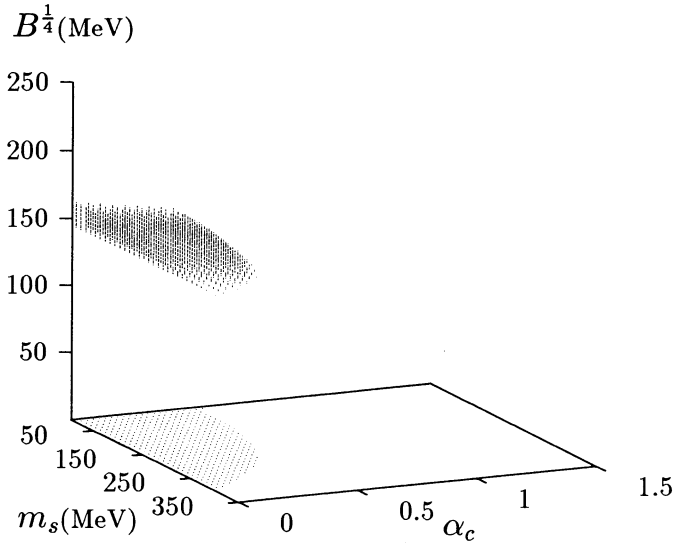

FIG. 11.—Parameter space for Q stars

space. The QNQN space lies directly above (in the $B^{1/4}$ axis) the QNQ space. This is due to the onset of a neutron phase at low pressure. Figure 11 presents the space for Q stars which lie below the QN quark parameter space in Figure 8. This is also due to a high pressure phase transition to N matter at the stellar core.

5. CONCLUSIONS

There is a fairly large region for Q, N, QN, and NQ stars, with neutron (N) stars dominating all the other classes. Hybrid stars (QN) with neutron exteriors comprise the second largest space and dominate pure quark stars. Surprisingly, NQ stars also occupy a larger part of the quark parameter space than pure quark stars do. Not unexpectedly, the more exotic stellar classes (QNQN, QNQ, and NQN) take up less than 2% of the total quark parameter space.

Observational testing may be possible. At low mass, one may be able to distinguish between stars with neutron matter or quark matter at low density via observations of coalescing neutron and black hole binaries (Cutler et al. 1992). These observations are unlikely to be useful in dealing with large mass binaries where the all sequences have a similar form (see Fig. 3). On the other hand, once masses and radii data for stellar sequences are available, one may be able to determine the equation of state for dense matter (Lindblom 1992).

This calculation can be improved in several ways. First, this calculation uses a value of $P_{\max}$ which is not correlated to the onset of instability directly. One could improve this calculation by calculating P_{critical} for each value of the quark parameter space and use this value as $P_{\max}$.

Second, any particular class which is non-trivial contains all the subclasses that can be obtained by removing the core. A QN class also contains a pure N class. QNQN contains NQN, QN, and N classes. Thus, a more accurate "measure" for this space is needed. One possible solution is to take equal units of the mass for each sequence and calculate a point in the quark parameter space. This can be accomplished by generating sequences of stars which differ by some constant mass, assigning a value to each star. Obviously, both of these considerations can be integrated into the program simultaneously.

Finally, one could impose more restrictive values of the quark parameters and recalculate the quark parameter space. It could be that $\alpha_c \leq 1.0$ is the only valid regime in the quark parameter space, and so an m_s which reflects experimental values should be used.

I am grateful to John L. Friedman for his many suggestions and insights. I would also like to thank Robert R. Caldwell, Leonard Parker, A. V. Olinto, and F. Grassi for numerous comments and suggestions. Computer time was provided by National Center for Supercomputing Applications. This work was partially supported by NFS grant PHY-91-05935 and a US Department of Education Fellowship.

APPENDIX

THERMODYNAMIC POTENTIALS

The formulas for the thermodynamic potentials presented here are the same as those in Alcock et al. (1986):

$$\Omega_u = -\frac{\mu_u^4}{4\pi^2}\left(1 - \frac{2\alpha_c}{\pi}\right), \tag{A1}$$

$$\Omega_d = -\frac{\mu_d^4}{4\pi^2}\left(1 - \frac{2\alpha_c}{\pi}\right), \tag{A2}$$

$$\Omega_s = -\frac{1}{4\pi^2}\left[\mu A\left(\mu^2 - \frac{5}{2}m_s^2\right) + \frac{3}{2}m_s^4 \ln(F) - \frac{2\alpha_c}{\pi}\left\{[\mu A - m_s^2 \ln(E)]^2 - 2A^4 - 3m_s^4 \ln^2\left(\frac{m_s}{\mu}\right) + 6 \ln\left(\frac{\rho_r}{\mu}\right)[\mu m_s^2 A - m_s^4 \ln(F)]\right\}\right], \tag{A3}$$

$$\Omega_e = -\frac{\mu_e^4}{12\pi^2}, \tag{A4}$$

where $A = (\mu^2 - m_s^2)^{1/2}$, $F = (\mu + A)/m_s$, and $E = (\mu + A/\mu)$. The quantity ρ_r is taken to be 313 MeV as in Alcock et al. (1986).

REFERENCES

Alcock, C., Farhi, E., & Olinto, A. 1986, ApJ, 310, 261
Bartelski, J., Szymacha, A., Ryzak, A., Mankiewicz, L., & Tatur, S. 1984, Nucl. Phys. A, 424, 484
Benvenuto, O. G., Horvath, J. E., & Vucetich, H. 1991, Int. J. Mod. Phys., 6, 4769
Campbell, B., Ellis, J., & Olive, K. A. 1990, Nuc. Phys. B, 345, 57
Carlson, C. E., Hansson, T. H., & Peterson, C. 1983, Phys. Rev. D, 27, 1556
Chanowitz, M., & Sharpe, S. 1983, Nucl. Phys. B, 222, 211
Chin, S. A. 1978, Phys. Lett., 78B, 552
Cutler, C., et al. 1992, Caltech preprint GRP-316
DeGrand, T. A., Jaffe, R. L., Johnson, K., & Kiskis, J. 1975, Phys. Rev. D, 12, 2060
Ellis, J., Kapusta, J. I., & Olive, K. A. 1991, Nucl. Phys. B, 348, 345
Farhi, E., & Jaffe, R. L. 1984, Phys. Rev. D, 30, 2379
Freedman, B. A., & McLerran, L. D. 1978, Phys. Rev. D, 16, 1130
Glendenning, N. K. 1992, Phys. Rev. D, 46, 1274
Grassi, F. 1989, University of Illinois preprint 89–0816
Haensel, P., Zdunik, J. L., & Schaeffer, R. 1986, A&A, 160, 121
Lindblom, L. 1992, ApJ, 398, 569
Shapiro, S., & Teukolsky, S. 1983, Black Holes, White Dwarfs, and Neutron Stars (New York: Wiley-Interscience)
Wiringa, R. B., Fiks, V., & Fabrocini, A. 1988, Phys. Rev. C, 38, 1010
Witten, E. 1984, Phys. Rev. D, 30, 2